Metrol. Meas. Syst., Vol. 32 (2025) No. 3, pp. 1–15
DOI: 10.24425/mms.2025.155798

PAN
POLSKA AKADEMIA NAUK

METROLOGY AND MEASUREMENT SYSTEMS

Index 330930, ISSN 0860-8229
www.metrology.wat.edu.pl

ANALYSIS OF IMPACT OF MEMS ACCELEROMETER POSITIONING ON VIBRATION SENSOR PERFORMANCE

Wojciech Staszewski, Adam Jabłonski

AGH University of Krakow, Faculty of Mechanical Engineering and Robotics, al. A. Mickiewicza 30, 30-059 Krakow, Poland (✉ *wojciech.staszewski@agh.edu.pl*),

Abstract

This paper aims to present an approach to optimising MEMS-based vibration sensors by strategically placing the accelerometer to maximise the sensor's performance. Optimisation requires establishing specific criteria, and in this case, the objective is to maximise SNR, which is crucial for ensuring accurate and reliable measurements. In practical applications, vibration signals received by sensors can be highly complex, often containing a cyclic fault signature that is distorted by the transmission path. In addition, signals are frequently obscured by noise from other sources, reducing overall SNR. Addressing these issues, sensor placement becomes critical, as different positions in the structure can either amplify or decrease fault signatures that are essential for diagnosis. In the past, MEMS vibration sensors were efficient only for low frequency bands. The selected MEMS sensor has a linear frequency response range up to 11 kHz, so research focused on maintaining the linear response in our range of interest, and therefore the sensor design proves the ability to cover a wide frequency band. Having such a MEMS sensor enables one to create Condition Monitoring (CM) for early detection of various faults. One of the problems in realisation of a sensor is the design of the mechanical part so that the vibrations of machinery are properly transmitted in the frequency band of a sensor. Equally important is finding a location within the sensor to achieve an optimal signal transfer path. Ultimately, this optimisation aims to provide a robust solution for diagnostics, making MEMS-based sensors a viable alternative to piezoelectric sensors in industrial environments.

Keywords: Condition Monitoring (CM), Industry 4.0, MEMS, position analysis, vibration sensor.

1. Introduction

Nowadays, simulation techniques are an integral part of the design process and manufacturing technology. The current tendency in manufacturing forces the industry to produce lighter, more durable, easier to produce, and cheaper pieces of equipment. This is why *Finite Element Analysis* (FEA) becomes a key simulation method. The idea behind FEA is to break down a large structure with a high degree of complexity into smaller and more manageable sections called elements. Each element represents the mechanical properties of its local domain. By dividing the considered structure into smaller and smaller pieces, it is possible to gain an understanding of how the larger structure will respond to external or internal stimulation [1].

Article history: December 9, 2024; revised January 30, 2025; accepted July 25, 2025; available online August 6, 2025.

Micro electromechanical systems (MEMS) technology is commonly used to produce various micro devices such as micro sensors, micro actuators, and micro bandpass filters, and so on. MEMS-based devices are preferred in sensor design due to small size, minimal invasive implantation, material compatibility, and low power consumption [2].

The modern condition monitoring system based on MEMS sensors can reduce the installation costs per node by an order of magnitude [3], which is attractive, but that is not all. MEMS also provide extraordinary attributes such as size, weight, power consumption, and level of functionality [4]. The capability of such sensors allows for interconnecting different interfaces and simplifying their implementation.

Right now, one can say that humanity is in a MEMS era during which, after a phase driven mainly by systems miniaturisation, the augmented capabilities are added to microsystems: for instance, multi-axis measurement systems combining accelerometers, gyroscopes, pressure and magnetic field sensors. In the near future, we might witness a new phase in which microsystems will be included in wireless sensor networks (Internet of Things) and will have extra abilities and performances, such as energy autonomy and high reliability, even in extremely aggressive environments. After a period during which microsystems were the subject of research in academic laboratories, the MEMS industry started to appear on the market. Recently, the production of MEMS has expanded, mainly due to the needs of inertial MEMS (micro-accelerometers and micro-gyroscopes) in consumer products (mainly smart devices, such as smartphones) [5].

The optimisation of MEMS accelerometers is a critical area of research aimed at enhancing their performance and reliability in diverse applications. Numerous studies have explored different methodologies to achieve this goal, each addressing specific challenges associated with MEMS accelerometer design and deployment. The work done within the last few years highlights the importance of optimal placement in structural health monitoring, where sensor positioning significantly affects the accuracy of damage detection [6]. Similarly, scientists have recently focused on optimising the operational bandwidth of MEMS accelerometers in challenging environments, ensuring accurate signal acquisition even in the presence of fluid damping effects [7].

On the other hand, research such as *"Design Optimization of MEMS Comb Accelerometer"* and *"A Novel Design Methodology for the Mixed-Domain Optimization of a MEMS Accelerometer"* delves into the optimisation of structural and mixed-domain parameters to improve sensitivity, linearity, and mechanical stability [8, 9]. These studies emphasise the importance of integrating multiple domains – mechanical, electrical, and thermal – to achieve a more holistic improvement in sensor performance.

These diverse approaches collectively highlight the multi-faceted nature of MEMS accelerometer optimisation, addressing design, placement, and environmental resilience to deliver high-performance solutions across various industrial and scientific applications. This growing body of research underscores the critical role of optimisation in the advancement of MEMS accelerometer capabilities, making them more versatile and reliable for complex tasks such as condition monitoring, structural health evaluation, and precision instrumentation.

2. Advantages of MEMS accelerometers

MEMS accelerometers are developing rapidly and hold a significant promise for a wide range of applications, particularly in industries requiring precise vibration and motion sensing. These sensors, built using MEMS technology, are not only compact and cost-effective [10], but also provide high levels of integration [11], making them ideal for mass production. Their continuous improvement has resulted in improved signal-to-noise ratios, broader frequency response ranges, and lower power consumption, making them competitive with more traditional sensor technologies such as piezoelectric accelerometers. In addition, their versatility allows for use in various environments, from consumer electronics to industrial machinery monitoring and diagnostics. In this section, we will explore the key advantages that make MEMS accelerometers increasingly attractive in modern sensing applications. Typical MEMS have two main features:

- design at the micro- or nanoscale,
- involvement of multiple physical domains (like mechanics, electronics, informatics).

These systems are designed in such a way as to interact with the environment either in a sensing or actuation mode to generate state information or control it at a different scale [12, 13]. MEMS, semiconductors, and *integrated circuits* (ICs) are based on silicon wafer fabrication technology, but MEMS add the dimensions of space. Some of the key advantages of MEMS are [14]:

- the ability to miniaturise physical interactions to nearly the same degree as IC's,
- low-cost mass production,
- simple to incorporate into more complex systems,
- good thermal properties,
- reduced size of the element,
- low power consumption,
- resistant to shock, radiation, and vibration,
- integrate sensing, analysis, and response.

Focusing on vibration sensors, as MEMS are low-cost and manifest high accuracy while having a relatively low noise to signal ratio, they are used in a range of applications, from educational to scientific and industrial purposes. Their advantages are mainly reflected in the following aspects:

- small sensor size combined with high measurement accuracy – MEMS sensors are compact, making them ideal for applications where space is limited, while still providing precise measurements across a wide range of conditions,
- high degree of integration, resulting in mass-production capability – The ability to integrate MEMS sensors into electronic systems facilitates cost-effective mass production, making them more accessible for a wide range of applications,
- improved signal-to-noise ratio in newer designs – Recent advancements in MEMS technology have significantly improved the signal-to-noise ratio, narrowing the performance gap between MEMS accelerometers and traditional piezoelectric accelerometers,
- wider frequency band in newer designs – Modern MEMS accelerometers can now handle a higher frequency range, making them more versatile in various monitoring and diagnostic tasks,
- much lower time constant compared to piezoelectric accelerometers – MEMS sensors exhibit a significantly faster response to changes in mechanical vibrations, offering more immediate feedback in dynamic environments,
- lower power consumption – MEMS sensors typically consume less power than their piezoelectric counterparts, making them more suitable for battery-powered or energy-efficient systems.

Rapid development of MEMS accelerometers paired with the improvement of their properties results in new application prospects regarding vibration sensors. These advancements have led to significant improvements in measurement accuracy, reliability, and signal-to-noise ratio, making MEMS-based accelerometers increasingly suitable for industrial monitoring applications. Furthermore, the miniaturisation and cost reduction associated with MEMS technology open new possibilities for large-scale deployment in complex machinery systems, where traditional sensors may have been too costly or cumbersome [15].

The data presented in this study align closely with industry standards and commonly observed characteristics of MEMS-based accelerometers, as described in both catalogue data and the scientific literature. MEMS accelerometers, such as those produced by Analog Devices (*e.g.*, ADXL1001 and ADXL356 series), serve as references for evaluating the performance of our proposed sensor design. Catalogue specifications highlight key performance metrics such as bandwidth, noise density, dynamic range, and linearity, all of which are critical to assessing the suitability of these sensors for condition monitoring applications. For instance, the ADXL1001 accelerometer offers a wide bandwidth of up to 10 kHz and a low noise density of 25 $\mu g/\sqrt{Hz}$, making it a popular choice for vibration analysis [16]. Similarly, the ADXL356 series provides a trade-off between cost and performance, with bandwidths up to 5 kHz and a noise density of 80 $\mu g/\sqrt{Hz}$. These figures form the baseline for evaluating the s*ignal-to-noise ratio* (SNR) improvements in our design.

The scientific literature corroborates the relevance of these catalogue data and provides additional insights into the optimisation of MEMS accelerometers. For example, in *Bandwidth Optimization of MEMS Accelerometers in Fluid Medium Environment* [7], the authors discuss how design alterations, including placement and packaging, can significantly influence bandwidth and noise performance. Similarly, the study *Robust Optimization of a MEMS Accelerometer Considering Temperature Variations* [17] explores how environmental factors, such as temperature and structural resonances, impact the reliability of an accelerometer, emphasising the importance of simulation-driven design to mitigate these issues. By integrating catalogue data and leveraging findings from these studies, our design approach strategically positions the MEMS element on a *printed circuit board* (PCB) to balance manufacturability, cost, and performance.

3. MEMS-based sensor design – location of accelerometer

The location of the sensor and its installation are two of the important parts of vibration data collection, which is why the acquisition point must be chosen considering some criteria. This place in the machine, called the reading point, is critical for obtaining accurate measurements of the machine's dynamic behaviour. General guidelines on vibration sensor location and mounting requirements are provided in the ISO 20816 standard, which outlines best practices to ensure reliable and consistent data. Proper sensor positioning and mounting according to these guidelines can significantly impact the effectiveness of condition monitoring and fault detection systems. The rotating machinery generates vibrations by means of cyclic internal forces that cannot be directly measured. The diagnostic procedures are based on the measurement of transmission of those forces through the structure of the machine (for instance, its chassis) and therefore the vibration sensor measures the response of those elements. The main reason for proper selection of the reading point is to minimise the effects of this mechanical excitation (of its parts and entire structure, as well) since the point of interest is in measuring the internal cyclic forces. That is why it is crucial to carefully consider the location of the MEMS accelerometer within the sensor housing, as optimising its placement can significantly reduce signal distortion and noise, thereby and maximise SNR and enhance the sensor's ability to accurately detect cyclic fault signatures. Fig. 1 presents the proposed simplified designs of an accelerometer with a MEMS sensor located in various parts of the PCB board.

The numerical FEM analysis was conducted using a detailed model that incorporates the mechanical properties of both the PCB and its metal support. The PCB was modelled as a composite structure with a Young's modulus of 24 GPa, a density of 1850 kg/m^3, and a Poisson's ratio of 0.136, while the bottom support was made of metal with a significantly higher stiffness (Young's modulus of 193 GPa), a density of 8000 kg/m^3, and a Poisson's ratio of 0.29. To accurately capture the structural behaviour, a tetrahedral mesh was employed with an adaptive size function and a minimum edge length of 4.3742e-4 m, ensuring sufficient resolution of critical features. The imposed constraints reflected the real-world assembly conditions: the PCB was tightly fitted into the metal support, and the support itself was fixed to the machine via a screw connection. This boundary condition effectively constrained the lower part of the assembly, simulating a rigid attachment and allowing the upper part of the PCB to deform freely under external forces and vibrations. These constraints played a crucial role in the modal analysis, influencing the natural frequency distribution and the mode shapes observed in the simulation.

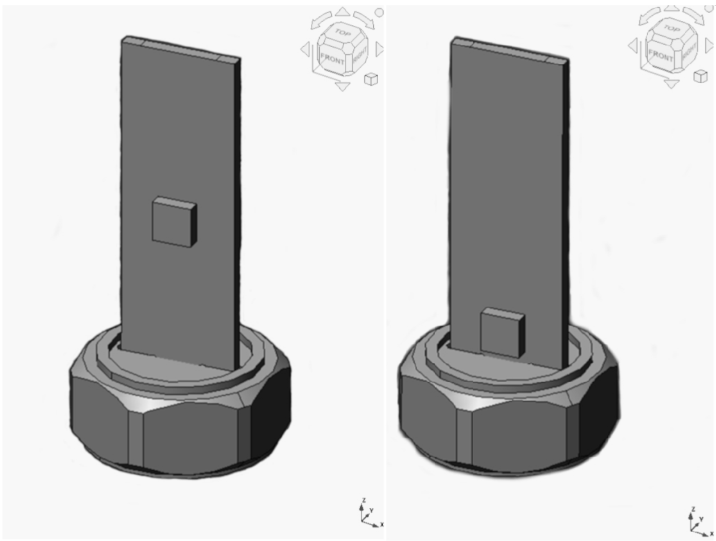

Fig. 1. Considered locations of a MEMS sensor on the PCB board of the accelerometer.

Next, FEM analysis was used to simulate the excitation of the sensor board under load (1 [g]) in the Z direction, i.e., the axis of measurement of the MEMS accelerometer. Since the sensor has the linear frequency response range up to 11 kHz, the analysis was performed in a range between 100 Hz and 10 kHz.

Table 1 presents the results of the modal analysis performed for two potential locations of the MEMS transducer on the sensor's PCB, at the bottom and middle positions. The objective of this analysis was to evaluate whether repositioning the MEMS transducer could shift the resonant frequencies to a higher range, thus achieving a more linear response in the lower frequency range. The entry for Mode 1 with 0 Hz frequency at both sensor locations indicates that no vibrational mode is excited in this configuration. This is likely due to the constraints and boundary conditions of the model, which prevent any resonance at this mode. For the bottom location, the resonant frequencies increase significantly across the modes, particularly in the higher modes (*e.g.*, 9,856.50 Hz for Mode 7 and 30,664.00 Hz for Mode 11). In contrast, the middle location demonstrates generally lower resonant frequencies, especially in the higher modes (*e.g.*, 1,085.00 Hz for Mode 7 and 13,965.00 Hz for Mode 11). These findings suggest that positioning the MEMS transducer at the bottom of the PCB shifts the resonant frequencies to higher values, contributing to a more desirable linear response in the lower frequency range, which is critical for accurate vibration measurement in practical applications.

As a simplification, a 3% damping ratio was introduced in order to resemble the real damping of the structure. This value was chosen to approximate the behaviour of real-world materials and connections where energy dissipation through internal friction or external resistance plays a significant role. By introducing this damping ratio, the model better reflects the dynamic response of the system under operating conditions, ensuring more realistic simulation results. Fig. 2 presents the obtained frequency response for a sensor with MEMS located in the middle of the PCB board and Fig. 3 presents the obtained frequency response for a sensor with MEMS located on the bottom of the PCB board.

Table 1. Obtained results from modal and harmonic analysis for two considered MEMS locations.

	Frequency [Hz]	
Mode	**Location: Bottom**	**Location: Middle**
1	0	0
2	1.32	2.64
3	44.16	1.24
4	127.63	113.21
5	201.65	138.57
6	3309.50	247.66
7	9856.50	1085.00
8	18 115.00	4460.00
9	20 350.00	5492.00
10	28 831.00	8018.00
11	30 664.00	13 965.00
Resonance	**Location: Bottom**	**Location: Middle**
1	3178.90	931.60
2	9841.00	5416.30

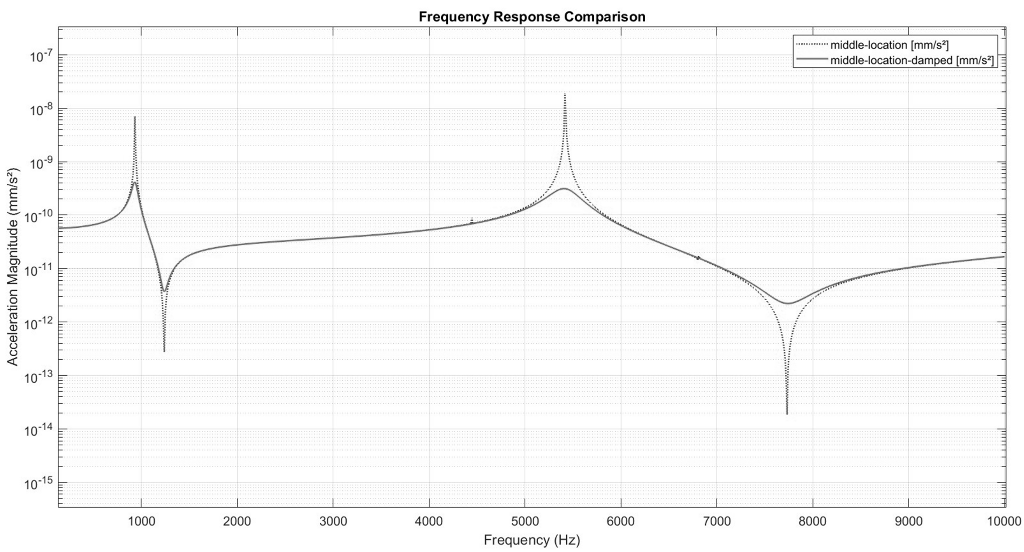

Fig. 2. Frequency response of a sensor with a MEMS located in the middle of the PCB board.

DOI: 10.24425/mms.2025.155798

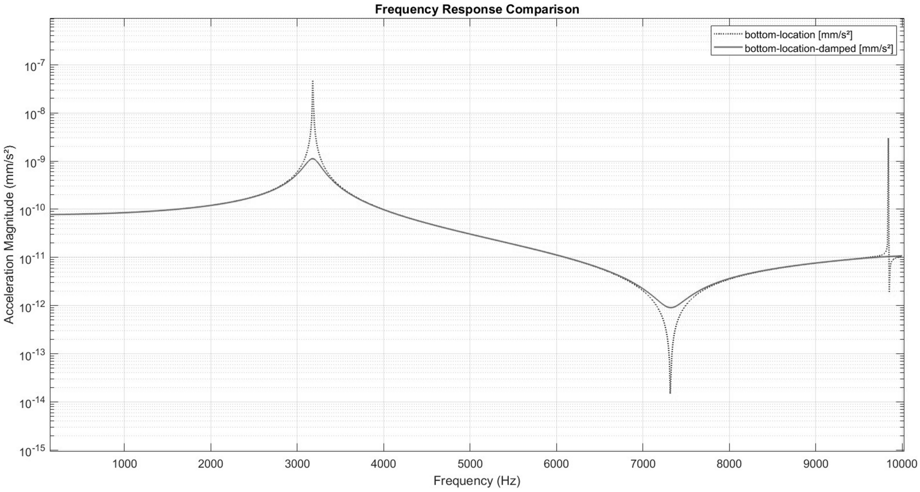

Fig. 3. Frequency response of a sensor with MEMS located on the bottom of the PCB board.

The results obtained prove that the relation between the accelerometer position and the mounting point directly influences the mechanical excitation effects of the entire structure, which is reflected in acceleration measurement. Specifically, comparing the two configurations – where the accelerometer is located at the bottom versus the middle of the sensor's PCB board – shows significant differences in the frequency response of the system. Although positioning the accelerometer at the bottom of the board may seem intuitive, it posed significant challenges in the prototype manufacturing process, making it more expensive to implement due to technological constraints. Additionally, the location at the bottom was initially complicated by a topological issue as nearby electronic components caused interference, requiring careful adjustments to mitigate these disturbances. Despite these difficulties, the results clearly indicate that the bottom position is a rational choice, as it allowed a better shift of resonance to higher frequencies, extending the effective frequency range of the sensor. A comparison of results for the damped structure is presented in Fig. 4.

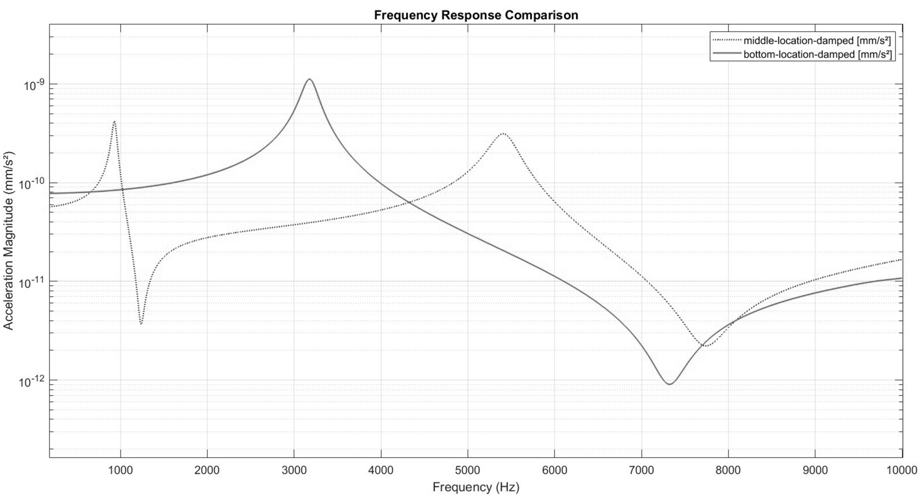

Fig. 4. Comparison of the structure frequency response depending on the location of the MEMS on the PCB board.

The preliminary harmonic analysis of the mechanical model showed potential resonances within the range of the accelerometer bandwidth. During the simulation, it was found that in the range of 1 Hz to 10 kHz there might be two potential resonances around ~1 kHz, ~5.5 kHz for the 'middle' design and around ~3 kHz, ~10 kHz for the 'bottom' design. This indicates that repositioning the MEMS accelerometer can significantly increase the resonant frequencies of the structure (for the considered mechanical design), which is desirable for achieving higher resonance limits. However, even at current resonant frequencies, the sensor would still meet the ISO VRMS standards. To verify the validity of the model, the experiment was planned and conducted.

4. Static analysis using acoustic excitation and vibration shaker

This chapter describes the experiments that were conducted to validate the model used for the simulations. In order to do so, a prototype PCB board with a MEMS accelerometer located on the bottom of the board (the case of the MEMS located closer to the mounting point of a sensor) was developed. Table 2 presents the technical parameters of the chosen accelerometer [16].

Table 2. Technical specification of the MEMS accelerometer chosen for the sensor prototype.

Parameter	**MEMS:** ***ADXL1001***	**Unit**
Measurement Range	±100	g
Sensitivity	20	mV/g
Noise Density	30	$\mu g/\sqrt{Hz}$
Sensor Resonant Frequency	21	kHz
Linear Frequency Response Range	up to 11	kHz
Operating Temperature	–40, +125	°C

4.1. Measurement with a PCV400 laser vibrometer

In order to prove the correctness of the simulations, an experiment was conducted during which a laser vibrometer was used to measure the vibrations of the considered structure. Since the vibrometer outputs the velocity of vibrations, the velocity data from the simulation was considered (the simulation was conducted for displacement, velocity, and acceleration of vibrations). Fig. 5 presents the test bench used during this experiment. As a source of excitation, an audio speaker was used.

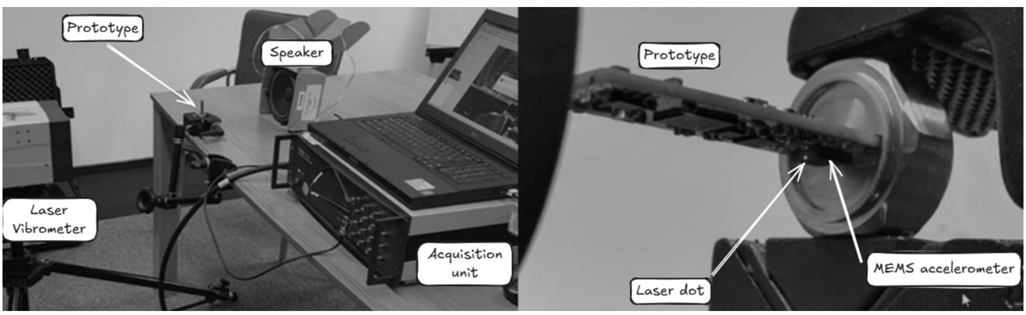

Fig. 5. Experiment set-up using a Polytec PSV400 laser vibrometer – left-hand side picture. Laser beam pointed to the face of the accelerometer in the direction of the measurement – right-hand side picture.

Results obtained from the experiment (presented in Fig. 6) in comparison with FEM analysis indicate that the simulated shape of frequency response, especially the location of assumed resonance around 3–3.5 kHz, is manifested in both simulation and experiment results. In fact, it was not possible to excite the system properly with a speaker in the spectrum between 100 Hz and 10 kHz, but the obtained results suggest that the simulation might be valid and, therefore, the hypothesis that the closer the MEMS to the mounting point of the sensor, the less it is affected by unwanted effects of vibration propagation might be valid as well.

The results obtained indicate that positioning the MEMS accelerometer closer to the mounting point of the sensor can move the two characteristic resonances that were found during the simulation to the higher frequency range. As it is not possible to apply the load in a broad frequency spectrum from a single speaker, other sources of excitation must be used in further experiments.

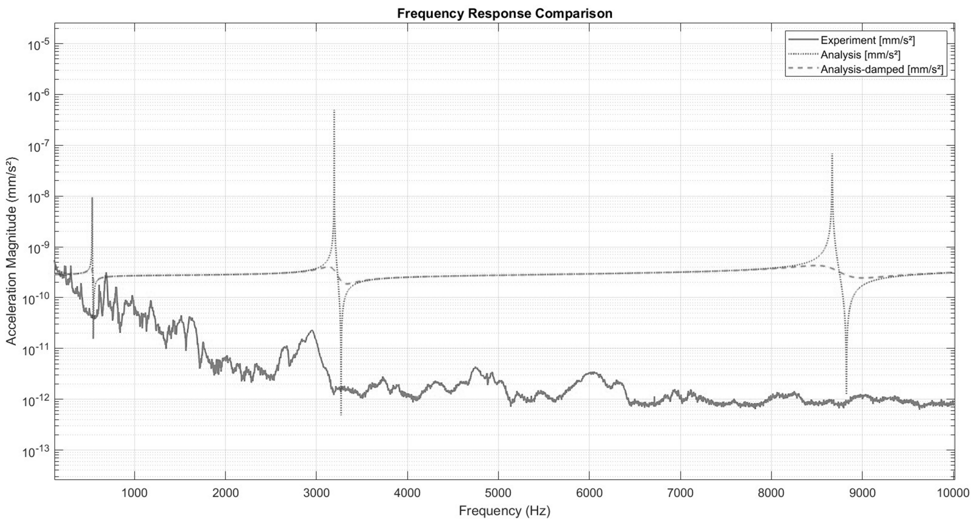

Fig. 6. Comparison of the frequency response obtained from the analysis (calculated for velocity in [m/s]) and the experiment using the PSV400 laser vibrometer.

4.2. Measurements with the reference sensor on a TIRAvib TV51144 shaker

Since the results of the previous experiment indicated that our assumption is correct, we set up another experiment in which we were able to control the input signal more directly. In order to achieve it, a TIRAvib TV51144 shaker was used. Figure 7 presents the test bench used during this experiment. The shaker was used as a source of excitation, and an additional piezoelectric sensor was used as a reference. Although the acoustic excitation experiment was not successful, it provided an initial indication that optimising the placement of MEMS on the PCB can significantly influence the quality of the data.

The results obtained from the experiment are presented in Fig. 8. The top graph shows the reference sensor, and the bottom graph presents the MEMS accelerometer. The results show that the shaker has some mechanical imperfections that are visualised by ‘glitches’ on the reference signal graph. The resonant frequency of the shaker is supposed (according to technical specs) to be around 6.5 kHz, but it is possible to observe that resonance is at 5–5.5 kHz (it starts already at around 4.5 kHz).

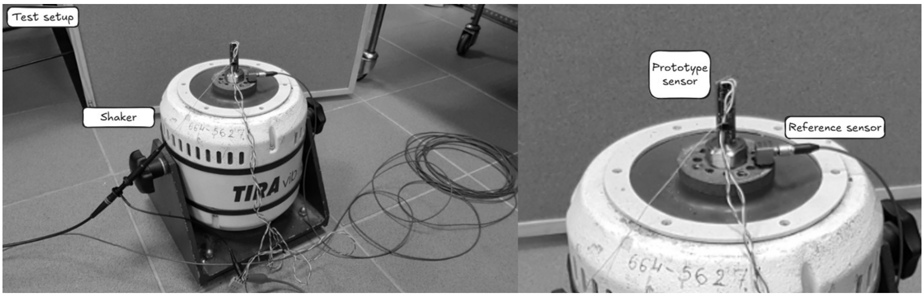

Fig. 7. Experimental setup using a TIRAvib TV51144 shaker and a reference sensor.

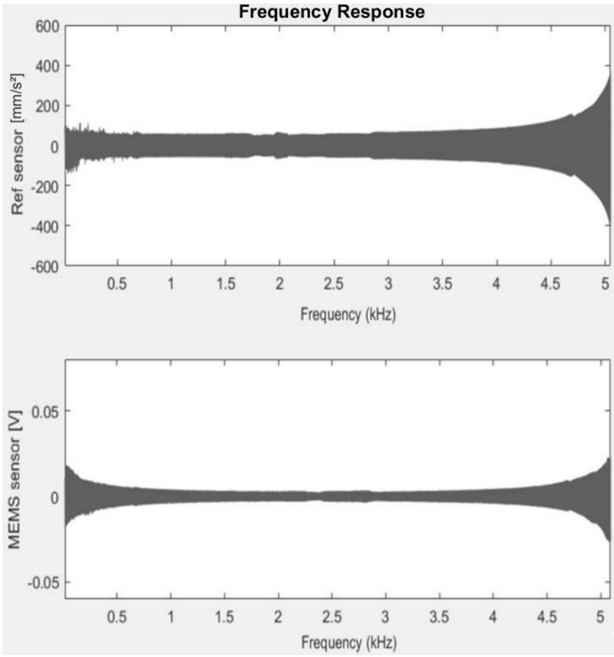

Fig. 8. Raw signal (time-series) measured from the reference and MEMS sensors on the TIRAvib TV51144 shaker.

Figure 9 presents the *Frequency Response Function* (FRF) calculated in MATLAB from the signal measured by the MEMS accelerometer (a rectangular window of 100 ms was used in the calculations). The top subplot displays the phase response of the system as a function of frequency, and the bottom subplot shows the magnitude of dynamic flexibility (a measure of system response) on the logarithmic scale – left Y-axis, alongside coherence as an additional indicator of signal quality – right Y-axis.

The sensitivity drop above 6.5 kHz is related to the characteristics of the TIRAvib TV51144 shaker. It has an upper frequency range of 6.5 kHz, but around 5.5 kHz, we observed a resonance of the shaker itself. Therefore, we were unable to conduct studies across the entire sensor range and focused only on frequencies up to 5 kHz.

The FRF obtained is stable up to 5 kHz, indicating that the simulated resonance (~3 kHz) for the 'bottom' location of the MEMS accelerometer is not present in the experimental results. This discrepancy suggests that while simulations can predict potential resonance frequencies, they

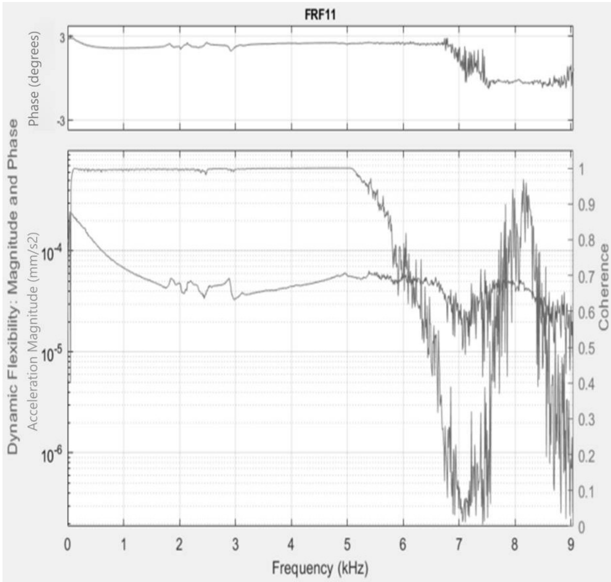

Fig. 9. Frequency response calculated from the measured signal from the MEMS sensor on the TIRAvib TV51144 shaker.

may not fully capture all real-world boundary conditions and damping mechanisms. Theoretical models often assume idealised conditions, omitting factors such as internal damping effects introduced during PCB manufacturing, the influence of additional electronic components, and localised stiffness variations due to soldering and PCB layering. These unmodeled effects can dissipate vibrational energy, effectively suppressing resonances that were prominent in simulations. Consequently, while simulation remains a useful tool for identifying potential resonance points, the actual sensor structure and its interactions with surrounding elements significantly alter the final frequency response.

5. Comparative analysis of the signal-to-noise ratio between the prototype and the reference sensors

In this section, a comparative analysis of SNR was performed across the entire measurement loop, including the sensor, the wiring, and the acquisition system. The objective of these measurements is to evaluate the performance of a prototype MEMS-based vibration sensor in relation to a reference piezoelectric sensor. By comparing both systems, the aim is to quantify the impact of different sensor technologies on SNR, which directly influences the accuracy and reliability of vibration data. The tests were conducted under identical conditions, with both sensors connected to the acquisition setup. This approach allows to objectively assess the benefits and limitations of the MEMS sensor in terms of noise rejection and signal fidelity, which are critical factors in detecting machinery faults in real-world industrial environments.

Table 3 presents the measured levels of SNR for the prototype MEMS sensor compared to the reference piezoelectric (PCB) sensor across three axes of measurement: X, Y, and Z. As observed, the MEMS sensor does not demonstrate a lower level of intrinsic noise compared to the PCB sensor; for instance, the MEMS sensor exhibits an SNR of 0.0033 g in the Z-axis, whereas the reference sensor measures 0.0069 g. However, it should be noted that the latest generations of

MEMS sensors have achieved a significant reduction in intrinsic noise levels compared to their predecessors. This advancement suggests that modern MEMS sensors can be effectively utilised in diagnostic applications, as their SNR levels are comparable to those of traditional PCB sensors. Thus, the results indicate that while the performance of the MEMS sensor in terms of SNR is on par with that of the PCB sensor, the continued improvement in MEMS technology holds promise for future applications in machinery diagnostics.

Table 3. Measured levels of noise in the whole loop including sensors and acquisition units.

	MEMS: *ADXL1001 [g]*	**Reference [g]**
X: RMS(x – MEAN(x))	n/a	0.0042
Y: RMS(y – MEAN(y))	n/a	0.0114
Z: RMS(z – MEAN(z))	0.0033	0.0069

6. Conclusions

High frequency MEMS accelerometers have already been on the market for a few years [18]. They offered resonant frequencies up to 22 kHz and ±500 g range. Unfortunately, the high level of signal-to-noise ratio prevented the usage of such sensors in industrial applications. They were applied only for narrow band analysis, up to a frequency of 1 kHz [13]. Today, each year we can observe an improvement in the parameters of MEMS accelerometers, closing the gap between them and piezoelectric sensors [19].

The study carried out on the optimisation of low-cost MEMS-based accelerometer solutions demonstrates that strategic positioning of the accelerometer on the PCB sensor significantly enhanced its performance. By carefully selecting the placement based on the criteria aimed at maximising SNR, the effective operational range of the accelerometer was doubled. This finding aligns with the analysis presented in this paper, which emphasises the critical role of accelerometer positioning in improving the sensor's ability to detect machinery faults by mitigating noise interference and amplifying critical fault signatures. Although initially it was unknown that the placement of sensing elements in the sensor might drastically influence these measurement capabilities, the study proves the contrary and therefore it is important to conduct FEM analysis while designing key components of a Condition Monitoring System (CMS). Research shows that the concept of creating the condition monitoring system that includes MEMS-based accelerometers has the potential, and it is worth exploring, to bring the results of MEMS development into industrial applications [14].

The conducted analysis has revealed a significant quantitative improvement in the SNR of the prototype MEMS sensor compared to that of the reference sensor. By optimising the placement of the accelerometer and fine-tuning the sensor design, we achieved an approximate SNR improvement of 25%. The reported improvement was derived from a comparative analysis of measured acceleration signals obtained from the prototype MEMS sensor and the reference PCB sensor under identical test conditions. The improvement calculation is based on the root mean square (RMS) values of the signal components, where the noise level was determined by analysing the deviation of the acceleration signal from its mean value across multiple measurements. This improvement is largely due to the reduction of noise and interference caused by mechanical resonances, which were mitigated by shifting the placement of the sensing element. This more strategic placement allowed the sensor to deliver clearer and more reliable measurements, especially in the lower frequency bands. This improvement is largely due to the reduction of noise and interference caused by mechanical resonances, which were mitigated by shifting the placement of the sensing element. This more strategic placement allowed the sensor to deliver clearer and more reliable measurements, especially in the lower frequency bands. This improvement is largely due to the reduction of noise and interference caused by mechanical resonances, which were mitigated by shifting the placement of the sensing element. This more strategic placement allowed the sensor to deliver clearer and more reliable measurements, especially in the lower frequency bands.

A key outcome of this optimisation was the successful shift of the first resonant peak from approximately 0.5–1 kHz to a much higher frequency range of 3–3.5 kHz. This shift means that the sensor is now far less affected by resonance in the lower frequency range, resulting in a more linear and accurate response where early detection of machinery faults is critical. Additionally, the highest resonant peak, which initially occurred in the 5–5.5 kHz range, was entirely shifted beyond the measurement range. This effectively removes it as a source of interference, allowing the sensor to operate with improved stability and accuracy throughout the desired frequency band.

These modifications not only increase the usable frequency range of the sensor, but also improve its suitability for industrial applications, where reliable, low-noise measurements are critical for machinery condition monitoring and fault detection. The successful shifting of resonances ensures that the sensor can focus on relevant frequencies without distortion, offering a more effective solution for vibration analysis and early fault detection.

Optimisation of sensor placement also resulted in a notable reduction in the vibrations of the sensor's itself, decreasing them by approximately 8%. This reduction is a crucial factor in enhancing the overall performance of the sensor as part of a condition monitoring system. By minimizing self-induced vibrations, the sensor can now more effectively isolate and measure external mechanical vibrations from the machinery, leading to more accurate and consistent data acquisition. This improvement not only increases the sensor's durability but also enhances its reliability in long-term monitoring applications, making it a more robust and valuable component in industrial condition monitoring systems.

Acknowledgements

The authors express great appreciation to EC Test Systems Ltd. for providing access to the Polytec laser vibrometer as well as for their support during the process of experiment set-up and data measurement. We also extend our sincere gratitude to AMC Vibro Ltd. for granting us access to the Vibstand 2 test bench.

The paper is partially supported by grant No. FENG.01.01-IP.01-005/23 funded by the National Centre for Research and Development, Poland.

References

[1] Żur, P., Kołodziej, A., & Baier, A. (2019). Finite elements analysis of PLA 3D-printed elements and shape optimization. *European Journal of Engineering Science and Technology*, *2*(1), 59–64. https://doi.org/10.33422/ejest.2019.01.51

[2] Zargari, S., Falaki, S., & Veladi, H. (2016). Design and finite element analysis of a MEMS based capacitive pressure sensor using CNT/PDMS nanocomposite electrodes. In *24th Iranian Conference on Electrical Engineering (ICEE)* (pp. 1619–1623). https://doi.org/10.1109/iraniancee.2016.7585780

[3] Isermann, R. (2011b). Fault-Diagnosis Applications: Model-Based Condition Monitoring: Actuators, Drives, Machinery, Plants, Sensors, And Fault-tolerant Systems. In *Springer eBooks*. Springer Berlin, Heidelberg. https://doi.org/10.1007/978-3-642-12767-0

[4] Siddhpura, M., Siddhpura, A., & Bhave, S. (2008). Vibration as a parameter for monitoring the health of precision machine tools. In *International Conference on Frontiers in Design & Manufacturing Engineering (ICDM-'08), 01-02 February 2008*. Delhi: Macmillan.

[5] Corigliano, A., Ardito, R., Comi, C., Frangi, A., Ghisi, A., & Mariani, S. (2018). *Mechanics of Microsystems*. John Wiley & Sons. https://doi.org/10.1002/9781119053828

[6] Jiang, Z., & Gao, Y. (2018). Accelerometer optimization placement using improved particle swarm optimization algorithm based on structural damage identification. *IOP Conference Series: Materials Science and Engineering*, *466*, 012093. https://doi.org/10.1088/1757-899x/466/1/012093

[7] Xu, X., Wu, S., Fang, W., Yu, Z., Jia, Z., Wang, X., Bai, J., & Lu, Q. (2022). Bandwidth optimization of MEMS accelerometers in fluid medium environment. *Sensors*, *22*(24), 9855. https://doi.org/10.3390/s22249855

[8] Sharma, K., & Macwan, I. G., & Zhang, L., & Hmurcik, L., & Xiong, X. (2008, March), *Design Optimization of MEMS Comb Accelerometer* Paper presented at *2008 ASEE Zone 1 Conference*, West Point, NY. https://doi.org/10.18260/1-2-1153-53702

[9] Pak, M., Fernandez, F. V., & Dundar, G. (2018). A novel design methodology for the mixed-domain optimization of a MEMS accelerometer. *Integration*, *62*, 314–321. https://doi.org/10.1016/j.vlsi.2018.03.018

[10] Yang, Q., Cai, C., Yang, M., Kong, M., Liu, Z., & Liang, F. (2023). Dynamic tilt testing of MEMS inclinometers based on conical motions. *Metrology and Measurement Systems*, 30(1), 31–47. https://doi.org/10.24425/mms.2023.144398

[11] Korobiichuk, I. (2017). Analysis of Errors of Piezoelectric Sensors used in Weapon Stabilizers. *Metrology and Measurement Systems*, *24*(1), 91–100. https://doi.org/10.1515/mms-2017-0001

[12] Korvink, J. G., & Paul, O. (2006). MEMS: A Practical guide to design, analysis, and applications. In *Springer eBooks*. Springer Berlin, Heidelberg. https://doi.org/10.1007/978-3-540-33655-6

[13] Jha, A.R. (2008). MEMS and Nanotechnology-based Sensors and Devices for Communications, Medical and Aerospace Applications (1^{st}. Ed.). CRC Press. https://doi.org/10.1201/9780849380709

[14] Chen, Y. J. (2013). Advantages of MEMS and its Distinct New Applications. *Advanced Materials Research*, *813*, 205–209. https://doi.org/10.4028/www.scientific.net/amr.813.205

[15] Najafabadi, H. R., Goto, T. G., Martins, T. C., Tsuzuki, M. S. G., & Barari, A. (2024). Designing MEMS accelerometer for enhanced sensitivity and reduced cross-sensitivity in landslide monitoring. *Measurement*, *226*, 114092. https://doi.org/10.1016/j.measurement.2023.114092

[16] Analog Devices (2018) Specification of ADXL1001/1002 accelerometers. http://www.analog.com/media/en/technical-documentation/data-sheets/ADXL1001-1002.pdf Accessed 10 January 2024

[17] Liu, G., Yang, F., Bao, X., & Jiang, T. (2015). Robust optimization of a MEMS accelerometer considering temperature variations. *Sensors*, *15*(3), 6342–6359. https://doi.org/10.3390/s150306342

[18] Ratcliffe, C., Heider, D., Crane, R., Krauthauser, C., Yoon, M. K., & Gillespie, J. W. (2007). Investigation into the use of low cost MEMS accelerometers for vibration based damage detection. *Composite Structures*, *82*(1), 61–70. https://doi.org/10.1016/j.compstruct.2006.11.012

[19] Jabłoński A., & Staszewski W. (2019) *Sposób i urządzenie pomiarowo-transmisyjne do akwizycji danych pomiarowych układów mechatronicznych. [Method and the measuring-transmission device for acquisition of the mechatronic devices measuring data.]* (Polish patent No. 238650) Patent Office of the Republic of Poland. http://patenty.bg.agh.edu.pl/pelneteksty/PL423514A1.pdf (in Polish)

Metrol. Meas. Syst., Vol. 32 (2025), No. 3, pp. 1–15
DOI: 10.24425/mms.2025.155798

Wojciech Staszewski is an assistant professor in the Department of Robotics and Mechatronics of the Faculty of Mechanical Engineering and Robotics at the AGH University of Krakow, Poland. He graduated from the AGH University of Science and Technology (Bachelor – 2014, Master – 2015, PhD - 2024). His research focuses on the use of MEMS sensors for applications related to condition monitoring systems. He develops dedicated methods for digital processing of signals which enable the determination of indicators of the technical condition of rotating machines. He specialises in programming in C, C++, C#, JavaScript, Python and MATLAB, has extensive experience working with .NET framework.

Adam Jabłoński is an associate professors in the Department of Robotics and Mechatronics of the Faculty of Mechanical Engineering and Robotics at the AGH University of Krakow. After years of experience as a diagnostic engineer, he became a senior researcher in the field of condition monitoring systems of rotary machinery. He has authored nearly 100 publications in the field of condition monitoring systems, signal processing, and machine diagnostics and developed numerous pioneering signal processing methods. He graduated from Central Texas College (USA) with Highest Honours (2004) and from AGH University of Science and Technology (Bachelor – 2006, Master – 2008, PhD – 2013).